DOI: 10.1002/chem.200601148

Mechanistic Studies on Peroxide Activation by a Water-Soluble Iron(III)–Porphyrin: Implications for O–O Bond Activation in Aqueous and Nonaqueous Solvents

Maria Wolak[a, b] and Rudi van Eldik*[a]

Abstract: The reactions of a water-soluble iron(III)–porphyrin, [*meso*-tetrakis(sulfonatomesityl)porphyrinato]iron(III), [Fe^{III}(tmps)] (**1**), with *m*-chloroperoxybenzoic acid (*m*CPBA), iodosylbenzene (PhIO), and H_2O_2 at different pH values in aqueous methanol solutions at −35 °C have been studied by using stopped-flow UV/Vis spectroscopy. The nature of the porphyrin product resulting from the reactions with all three oxidants changed from the oxo–iron(IV)–porphyrin π-cation radical [Fe^{IV}(tmps$^{\bullet+}$)(O)] (**1**$^{++}$) at pH < 5.5 to the oxo–iron(IV)–porphyrin [Fe^{IV}(tmps)(O)] (**1**$^{+}$) at pH > 7.5, whereas a mixture of both species was formed in the intermediate pH range of 5.5–7.5. The observed reactivity pattern correlates with the $E^{\circ\prime}$ versus pH profile reported for **1**, which reflects pH-dependent changes in the relative positions of $E^{\circ\prime}_{Fe^{IV}/Fe^{III}}$ and $E^{\circ\prime}_{P\cdot+/P}$ for metal- and porphyrin-centered oxidation, respectively. On this basis, the pH-dependent redox equilibria involving **1**$^{++}$ and **1**$^{+}$ are suggested to determine the nature of the final products that result from the oxidation of **1** at a given pH. The conclusions reached are extended to water-insoluble iron(III)–porphyrins on the basis of literature data concerning the electrochemical and catalytic properties of [Fe^{III}(P)(X)] species in nonaqueous solvents. Implications for mechanistic studies on [Fe(P)]-catalyzed oxidation reactions are briefly addressed.

Keywords: enzyme models · O–O activation · peroxides · porphyrinoids · reaction mechanisms

Introduction

Experimental and conceptual aspects addressed here relate to studies on the mechanism of O–O bond activation by heme monooxygenases and their biomimetic models. A unique feature of the enzymatic systems is heterolytic O–O bond cleavage in the iron(III) hydroperoxide intermediates, which results in the formation of a high-valent oxo–iron(IV)–porphyrin cation radical [Fe^{IV}(P$^{\bullet+}$)(O)], a $2e^-$-oxidized iron–porphyrin capable of oxidizing organic substrates in a highly stereospecific manner.[1–3] As biomimetic models for heme oxygenases, the reactions of iron(III)–porphyrins with oxo-transfer oxidants such as peroxy acids (RC(O)OOH), iodosylbenzene (PhIO), organic peroxides (ROOH), and H_2O_2 have been extensively studied.[1–9] The mechanistic picture that emerged from these studies turned out to be a complex one. The mode of O–O bond cleavage (homolysis or heterolysis) in the [Fe(P)(OOR)] intermediates as well as the nature of the actual catalytically active species were shown to depend on a number of factors, such as the type of porphyrin catalyst and oxidant, the polarity and acidity of the solvent, and the axial ligation of the iron(III) center.[5–9] Despite extensive investigations, many ambiguities with regard to the mechanism of O–O bond cleavage and subsequent oxygen atom transfer to an organic substrate remain unresolved.[5,10]

We present herein the results of low-temperature UV/Vis spectroscopic studies on the reaction of a water-soluble iron(III)–porphyrin [Fe^{III}(tmps)] (**1**) (Figure 1), with the oxidants *m*-chloroperoxybenzoic acid (*m*CPBA), iodosylbenzene (PhIO), and H_2O_2 in aqueous methanolic solutions of varying pH. The results obtained are discussed with reference to data on the speciation[11] and electrochemical properties[12] of **1** as a function of pH. The conclusions reached

[a] Dr. M. Wolak, Prof. Dr. R. van Eldik
Institute for Inorganic Chemistry
University of Erlangen-Nürnberg
Egerlandstrasse 1, 91058 Erlangen (Germany)
Fax: (+49) 9131-85-27387
E-mail: vaneldik@chemie.uni-erlangen.de

[b] Dr. M. Wolak
Department for Inorganic Chemistry
Jagiellonian University
Ingardena 3, 30060 Krakow (Poland)

Supporting information for this article is available on the WWW under http://www.chemeurj.org/ or from the author.

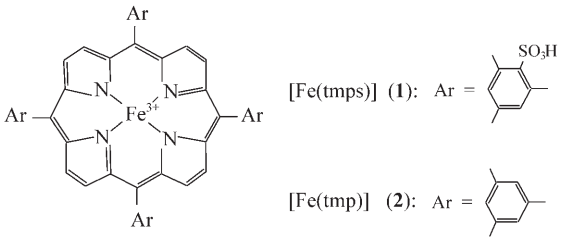

Figure 1. Structures of [Fe^{III}(tmps)] and [Fe^{III}(tmp)].

are extended to model water-insoluble iron(III)–porphyrins on the basis of reported literature data concerning the redox and catalytic properties of these systems.

Results and Discussion

Motivation for the choice of the system studied: The water-soluble complex **1** has a relatively electron-rich porphyrin ligand,[11,12] which (due to the presence of *ortho*-methyl substituents, Figure 1) prevents the formation of μ-oxo dimers[11] and imparts increased stability with respect to oxidative degradation (often encountered with other porphyrins lacking protective *ortho*-methyl groups).[12–14] These properties facilitate studies on the electrochemical and chemical oxidation of **1**.[12,13a] Moreover, the solubility of **1** in water provides a unique opportunity to study its redox properties as a function of pH and to relate these to its reactivity in catalytic oxidations at different pH values. The latter aspect is important in view of intriguing literature reports on the pH-dependent catalytic activity of water-soluble iron(III)–porphyrins in selected epoxidation reactions.[5m,n] The reactivity patterns observed in these studies[5m,n] were interpreted in terms of a pH-induced changeover in the mode of O–O bond cleavage in the [Fe^{III}(P)(OOR)] intermediates formed by peroxide binding to [Fe^{III}(P)], from heterolysis at low pH to homolysis at high pH. The possible reasons for such a mechanistic changeover were, however, not assessed. In our view, the reactivity observed originates from pH-dependent changes in 1) the speciation and/or 2) the electrochemical properties of [Fe^{III}(P)]. In an effort to resolve the mechanistic questions arising from the reported studies, we have chosen **1**, a complex well-characterized with regard to its speciation[11] and electrochemical properties[12] at different pH values, and have studied its reactions with the oxidants *m*CPBA, PhIO, and H_2O_2 as a function of pH, as described below.

Spectroscopic studies on the reactions of 1 with *m*CPBA, PhIO, and H_2O_2: As reported previously,[11a] the speciation of **1** in aqueous solutions in the pH range 0–13 is governed by the pH-dependent equilibrium shown in Equation (1a). In order to follow the reactions of **1** with the selected oxidants, the use of low temperatures (−30 to −40 °C) was necessary in order to stabilize and characterize the oxidized porphyrin products formed at various pH values. We therefore used a 4:1 (v/v) MeOH/H_2O mixture as a cryosolvent for the low-temperature spectroscopic studies. Spectrophotometric titration of **1** in this solvent mixture resulted in UV/Vis spectral changes closely resembling those previously observed in pure water (see Figure S1, Supporting Information). A pK_a of 6.3 ± 0.1 was determined for equilibrium according to Equation (1b) (see Figure S1, inset).[15,16]

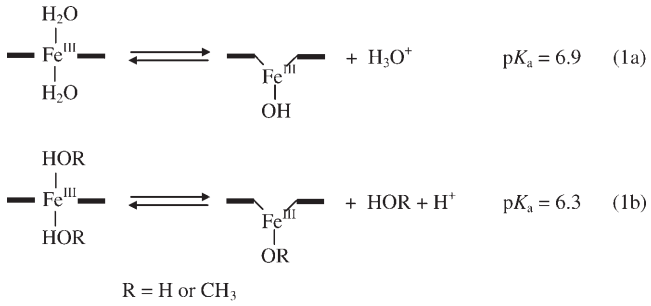

The reaction of **1** with *m*CPBA was followed by using low-temperature stopped-flow spectrophotometry at −35 °C. These studies clearly revealed a pH-dependent change in the nature of the products formed, as indicated in Figure 2. At pH < 5, the appearance of a product with a Soret band of decreased intensity at $\lambda = 404$ nm and a broad, low-intensity band with a maximum at around $\lambda = 670$ nm (Figure 2a) clearly indicated the conversion of **1**·H_2O to the oxo–iron(IV)–porphyrin cation radical [Fe^{IV}(tmps$^{\bullet+}$)(O)],[17] a 2 e^--oxidized form of **1** (abbreviated as $\mathbf{1}^{++}$ in the following text). In contrast, reaction at pH > 7.5 gave a product with a Soret band at $\lambda = 425$ nm and a low-intensity band at $\lambda = 545$ nm (Figure 2d), previously assigned to [Fe^{IV}(tmps)(O)][12,13] (the 1 e^--oxidized form of **1**, designated by $\mathbf{1}^{+}$ hereinafter). Clean isosbestic points indicated that at pH < 5.5 and pH > 7.5 the reaction involves a single spectroscopically observable step at −35 °C. The spectral changes observed in the intermediate pH range 5.5 < pH < 7.5 were indicative of the formation of a mixture of $\mathbf{1}^{++}$ and $\mathbf{1}^{+}$ as reaction products. The [$\mathbf{1}^{++}$]/[$\mathbf{1}^{+}$] ratio gradually decreased on increasing the pH, with $\mathbf{1}^{+}$ being the only observable product at pH > 7.5.

Because the pK_a of *m*CPBA (7.6)[18] coincides quite closely with the intermediate pH range in which its reactivity toward **1** was found to change, the observed reaction pattern could possibly reflect the difference in reactivity of RC(O)OOH and $RC(O)OO^-$ toward **1**. We thus performed similar pH-dependent studies in which **1** was oxidized with iodosylbenzene and H_2O_2 (which do not exhibit pH-dependent equilibria in the pH range 5–8). When PhIO was used as the oxidant, the pattern of spectral changes was fully analogous to that observed with *m*CPBA, indicating the formation of $\mathbf{1}^{++}$ and $\mathbf{1}^{+}$ at pH < 5.5 and > 7.5, respectively, and a mixture of $\mathbf{1}^{++}$ and $\mathbf{1}^{+}$ at 5.5 < pH < 7.5 (compare Figure 3a and b for UV/Vis spectral evolutions at pH 4 and 9). The use of H_2O_2 as the oxidant resulted in slow decomposition of **1** at pH < 5.5 (Figure 3c). However, the spectral changes observed in this pH range resembled those record-

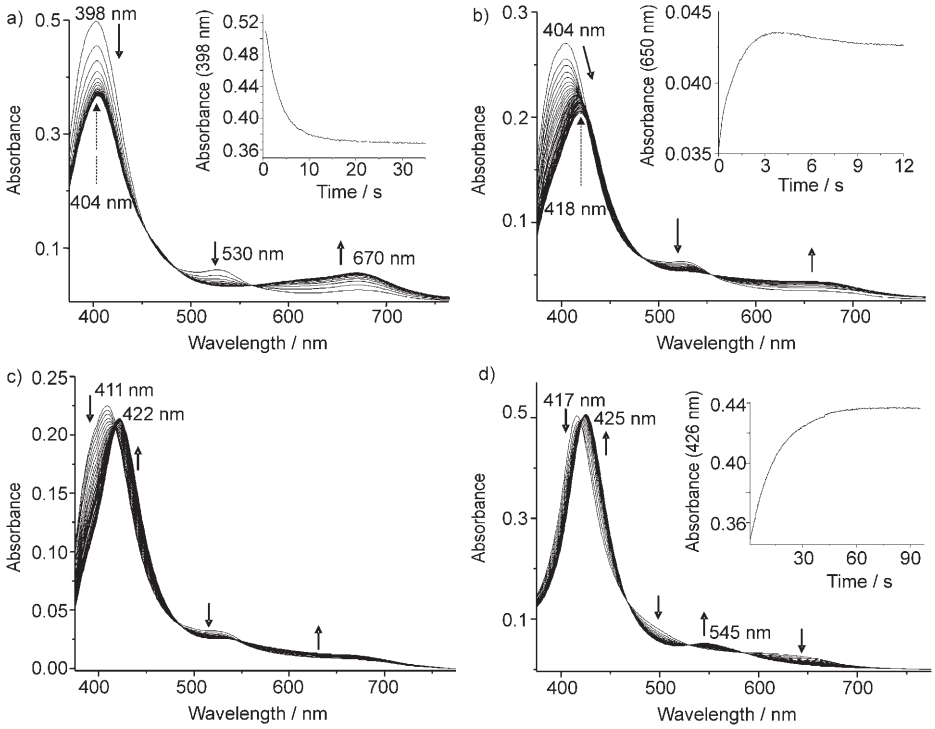

Figure 2. Spectral changes accompanying the reaction of *m*CPBA (1×10^{-3} M) with **1** ($\leq2\times10^{-5}$ M) in MeOH/H_2O (4:1) at selected pH values at −35 °C: a) pH 5.1, b) pH 6.5, c) pH 7.0, d) pH 8. (pH 5.1: MES buffer (0.01 M); pH 6.5–8: EPPS buffer (0.01 M).)

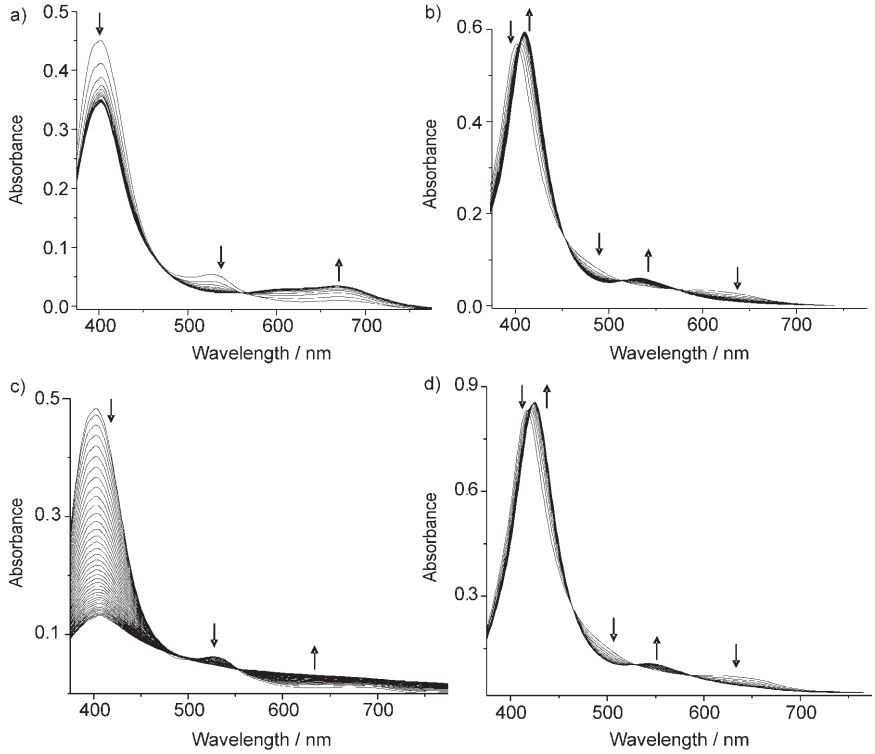

Figure 3. Evolution of UV/Vis spectra accompanying the reaction of **1** with PhIO (a, b) and H_2O_2 (c, d) in MeOH/H_2O (4:1, v/v) at −35 °C: a) 2×10^{-3} M PhIO, pH 4.0 (adjusted with HNO_3 in solutions of **1** and PhIO before mixing); b) pH 9.0 (0.01 M CAPS), 5×10^{-4} M PhIO; c) pH 5.0 (0.01 M MES), 0.1 M H_2O_2; d) pH 9.0 (0.01 M CAPS), 0.05 M H_2O_2.

ed for the reaction of **1** with a large excess of *m*CPBA at pH 5 (see Figure S2, Supporting Information), that is, under conditions that led to initial formation of $\mathbf{1}^{++}$ followed by porphyrin destruction by excess *m*CPBA. This suggests that decomposition of **1** by H_2O_2[19] at pH ≤ 5.5 involves initial formation of $\mathbf{1}^{++}$. As observed with *m*CPBA and PhIO, the spectral patterns that accompanied the reaction with H_2O_2 gradually changed in the pH range 5.5–7.5, and at pH > 7.5 indicated the formation of $\mathbf{1}^{+}$ in a single kinetically observable step (Figure 3d).

The aforementioned results reveal a consistent reactivity pattern for all three oxidants studied, in which $\mathbf{1}^{++}$ and $\mathbf{1}^{+}$ are the products at pH ≤ 5.5 and at pH > 7.5, respectively, and a mixture of $\mathbf{1}^{++}$ and $\mathbf{1}^{+}$ is formed in the intermediate pH range. This observation can be related to previous reports on pH-dependent changes in the catalytic activity of water-soluble $[Fe^{III}(P)]$ porphyrins,[5m,n] which pointed to a gradual change in the nature of the product formed upon oxidation of $[Fe^{III}(P)]$, from the catalytically active $2e^-$-oxidized form $[Fe^{IV}(P^{+\bullet})(O)]$ at low pH to the catalytically inactive $1e^-$-oxidized $[Fe^{IV}(P)(O)]$ at high pH. Our own measurements performed on **1** under catalytic conditions (oxidation of *cis*-stilbene by *m*CPBA in the presence of **1**) indicated efficient and stereospecific oxidation of *cis*-stilbene to *cis*-stilbene oxide at pH 5, which clearly proceeded through transient formation of $\mathbf{1}^{++}$ as the catalytically active species (see the Experimental Section). The catalytic activity of **1** was, however, completely lost at pH 8 (whereupon formation of $\mathbf{1}^{++}$ was not observed). These results conform

to the reactivity patterns described earlier[5m,n] for other water-soluble [Fe^{III}(P)] systems.[20]

Because the intermediate pH range in which the nature of the oxidized products formed by **1** gradually changed lies close to the pK_a of 6.3 characterizing the equilibrium according to Equation (1b), it could be suggested in a first approximation that the mechanism of oxidation of **1** is altered in response to a change in the axial ligation of **1** from [Fe^{III}(tmps)($ROH)_2$] to [Fe^{III}(tmps)(OR)]. In fact, several literature reports on water-insoluble [Fe^{III}(P)(X)]/ROOH systems have provided evidence of a significant influence of the axial iron ligation on the O–O bond cleavage mode in the [Fe(P)(OOR)(X)] species (as discussed in more detail later).[5f,j,k] Such an explanation, however, seems highly unlikely when data on the speciation of **1** as a function of pH are considered. Because only one pH-dependent equilibrium [Eq. (1a) or (1b), for water and MeOH/H_2O as solvent, respectively] is observed for **1** in the pH range 1–14, coordination of two negatively charged RO^- ligands (where R = H or CH_3) to the (relatively electron-rich) Fe^{III} center in **1** is evidently difficult and does not occur to any appreciable extent at [RO^-] ≤ 0.1 M. Thus, the formation of a [Fe^{III}(P)(OR)(OOR)] intermediate with two anionic axial ligands is highly unlikely in the studied pH range. Spectrophotometric titration data also indicate that coordination of ligands such as H_2O/MeOH (pK_a = 15.7 and 15.5, respectively) to the Fe^{III} center in **1** lowers their pK_a values by about 9 pH units (to a value of the order of 6.5–6.7) in water and in the aqueous methanol solvent employed. A similar shift of around 8 pH units has been estimated for H_2O_2 upon its coordination to the ferriheme center of peroxidase (pK_a(free H_2O_2) = 11.6; pK_a(coord. H_2O_2) ≈ 3.2–4).[21] It can thus be safely assumed that the pK_a values of the oxidants H_2O_2 and *m*CPBA (pK_a = 7.6)[18] decrease by around 8 pH units upon coordination to [Fe^{III}(tmps)]. This implies that the oxidant-bound intermediate formed by coordination of H_2O_2 and (in particular) *m*CPBA is deprotonated at pH > 4, as proposed in Scheme 1. No change in the axial ligation of the [Fe(tmps)(OOR)] intermediate (presumably a five-coordinate high-spin complex)[22] is therefore expected in the intermediate pH range of 5.5–7.5 in which the reactivity change is observed. The main conclusion from the reaction sequence in Scheme 1 is that although the change in the axial iron ligation in **1** [governed by Eq. (1a)/(1b)] is likely to influence the equilibrium constant *K* (initial oxidant coordination), it is not expected to influence the mode of the subsequent O–O bond cleavage, as the same [Fe(tmps)(OOR)] intermediate is involved in this step at pH > 4.

We propose that the observed reactivity pattern for the reaction of **1** with *m*CPBA, PhIO, and H_2O_2 results from pH-induced changes in the redox properties of **1** rather than its different ligation at low and high pH. The underlying rationale for this has come from consideration of the $E^{o\prime}$ versus pH diagram for electrochemical oxidation of **1** in aqueous solution depicted in Figure 4.[23] As shown in the diagram, oxidation of **1** may be porphyrin-centered (P → $P^{\bullet+}$) and/or metal-centered (Fe^{III} → Fe^{IV}). As the former does not involve release or uptake of protons, $E^{o\prime}_{P\bullet+/P}$ is relatively pH-insensitive.[24] This is in contrast to the pH-dependent Fe^{III} → Fe^{IV} oxidation, a process that is coupled to acid–base equilibria involving the formation of the oxo ligand. Due to the pH dependence of $E^{o\prime}_{Fe^{IV}/Fe^{III}}$, the relative positions of $E^{o\prime}_{Fe^{IV}/Fe^{III}}$ and $E^{o\prime}_{P\bullet+/P}$ and the nature of the most thermodynamically stabilized oxidized form of **1** change with pH. The diagram in Figure 4 can thus be divided into three sections, in which the first (thermodynamically most favored) oxidation is given by Equations (2)–(4), respectively.

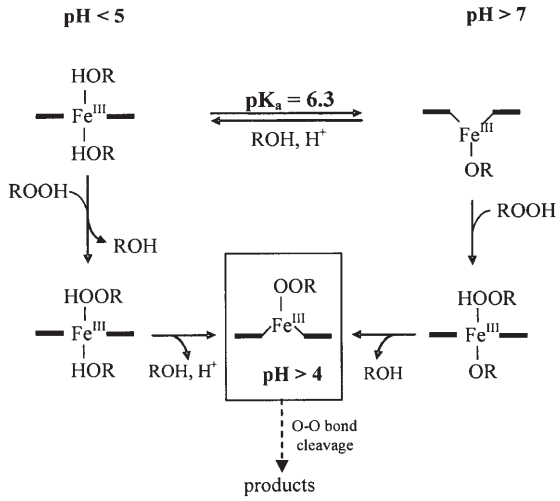

Scheme 1. Suggested reaction pathways for the formation of the [Fe(tmps)(OOR)] intermediate at low and high pH.

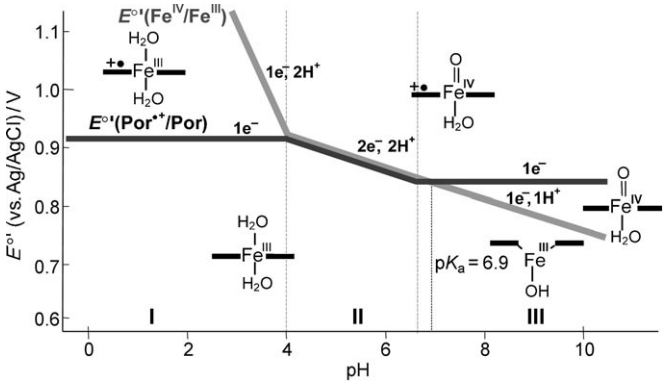

Figure 4. Schematic representation of the pH dependence of $E^{o\prime}$ for electrochemical oxidations of **1** in aqueous solution (constructed on the basis of data reported in ref. [12], see Figure S3, Supporting Information).

Section I (pH < 3.5)

$$[Fe^{III}(P)(H_2O)_2] \rightarrow [Fe^{III}(P^{\bullet+})(H_2O)_2] + e^- \quad (2)$$

Section II (3.5 < pH < 6.5)

$$[Fe^{III}(P)(H_2O)_2] \rightarrow [Fe^{IV}(P^{\bullet+})(O)(H_2O)] + 2e^- + 2H^+ \quad (3)$$

Section III (pH ≥ 7)

$$[Fe^{III}(P)(OH)] + H_2O \rightarrow [Fe^{IV}(P)(O)(H_2O)] + e^- + H^+ \quad (4)$$

In the context of chemical oxidation involving O–O bond cleavage of coordinated peroxide, the diagram in Figure 4 suggests that **1** as a redox partner may favor O–O bond homolysis ($1e^-$ oxidation) at pH < 3.5 and pH > 7, as in these pH ranges its $1e^-$ oxidation is thermodynamically most facile. In contrast, heterolysis of the O–O bond ($2e^-$ oxidation) should be favored in the pH range 4–7, in which $E^{\circ\prime}_{P^{\bullet+}/P} \approx E^{\circ\prime}_{Fe^{IV}/Fe^{III}}$. The mode of O–O bond cleavage is, however, expected to depend not only on the redox properties of **1** at a given pH, but also on the oxidative power of the oxidant. A strong oxidant (e.g., *m*CPBA) with $E^{\circ\prime}$ exceeding both $E^{\circ\prime}_{Fe^{IV}/Fe^{III}}$ and $E^{\circ\prime}_{P^{\bullet+}/P}$ may thus effect an initial $2e^-$ oxidation of **1** to $\mathbf{1}^{++}$ (O–O bond heterolysis) at pH > 7, while O–O bond homolysis ($1e^-$ oxidation to $\mathbf{1}^{+}$) should occur in this pH range for weaker oxidants with $E^{\circ\prime}_{Fe^{IV}/Fe^{III}} < E^{\circ\prime} < E^{\circ\prime}_{P^{\bullet+}/P}$ (such oxidants, however, may effect $2e^-$ oxidation of **1** at pH 4–7, either through direct O–O bond heterolysis or by two sequential $1e^-$ oxidations, due to the condition $E^{\circ\prime}_{Fe^{IV}/Fe^{III}} \approx E^{\circ\prime}_{P^{\bullet+}/P}$).

Importantly, the $E^{\circ\prime}$ versus pH dependence depicted in Figure 4 also implies the possible occurrence of redox equilibria involving comproportionation/disproportionation of high-valent iron–porphyrins, as shown in Equation (5) for the redox interconversion of $\mathbf{1}^{++}$ and $\mathbf{1}^{+}$.

$$2\,[Fe^{IV}(P)(O)] + nH^+ \underset{\text{compr.}}{\overset{\text{dispr}}{\rightleftharpoons}} [Fe^{IV}(P^{\bullet+})(O)] + [Fe^{III}(P)(L)] \quad K_{disp} \quad (5)$$

(low pH: $n = 2$ L = $2H_2O$; high pH: $n = 1$ L = OH^-)

The position of the equilibrium according to Equation (5) (i.e., the value of K_{disp}) depends on the difference between $E^{\circ\prime}_{P^{\bullet+}/P}$ and $E^{\circ\prime}_{Fe^{IV}/Fe^{III}}$ [Eqs. (5a)–(5c)], and (due to the $[H^+]$-sensitivity of the latter potential) is pH-dependent.

$$[Fe^{IV}(P^{\bullet+})(O)] + e^- \rightarrow [Fe^{IV}(P)(O)] \qquad E^{\circ\prime}_{P^{\bullet+}/P} \quad (5a)$$

$$[Fe^{IV}(P)(O)] + e^- + nH^+ \rightarrow [Fe^{III}(P)(L)] \qquad E^{\circ\prime}_{Fe^{IV}/Fe^{III}} = f(pH) \quad (5b)$$

Therefore, Equation (5) = [Eq. (5b)] − [Eq. (5a)], and

$$\log(K_{disp}) = (\Delta E^{\circ\prime})/0.059 \text{ (at } 25\,^\circ C) \qquad \Delta E^{\circ\prime} = E^{\circ\prime}_{Fe^{IV}/Fe^{III}} - E^{\circ\prime}_{P^{\bullet+}/P} \quad (5c)$$

It follows from Equation (5c) that in the intermediate pH range, in which $\Delta E^{\circ\prime}$ values are small, $\mathbf{1}^{++}$ and $\mathbf{1}^{+}$ may coexist in solution ($-0.059 < \Delta E^{\circ\prime} < 0.059$; $0.1 < K_{disp} < 10$), whereas for large $\Delta E^{\circ\prime}$ one of the redox forms ($\mathbf{1}^{++}$ when $E^{\circ\prime}_{Fe^{IV}/Fe^{III}} \gg E^{\circ\prime}_{P^{\bullet+}/P}$; $\mathbf{1}^{+}$ when $E^{\circ\prime}_{Fe^{IV}/Fe^{III}} \ll E^{\circ\prime}_{P^{\bullet+}/P}$) is strongly favored by the redox thermodynamics. For the present system, the occurrence of the pH-dependent equilibrium [Eq. (5)] was demonstrated in an independent experiment involving oxidation of **1** with *m*CPBA in MeOH/H_2O (4:1, v/v) at −35 °C. Addition of *m*CPBA (5×10^{-4} M) to a solution of **1** (1.2×10^{-5} M) in this solvent mixture at pH 4.5 led to the formation of a bright-green complex $\mathbf{1}^{++}$ (see Figure S4a, Supporting Information). Subsequent addition of hydroxide (7×10^{-4} M) resulted in conversion of $\mathbf{1}^{++}$ to $\mathbf{1}^{+}$ (Figure S4b). Upon addition of acid (HNO_3), the color reverted to the bright-green characteristic of $\mathbf{1}^{++}$ (the resulting UV/Vis spectrum was indicative of the formation of a mixture of $\mathbf{1}\cdot H_2O$ and $\mathbf{1}^{++}$). Several interconversions between $\mathbf{1}^{++}$ and $\mathbf{1}^{+}$ could be achieved by subsequent additions of acid and base (Figure S4c). Reported examples of analogous proton-dependent redox equilibria involving various oxidized forms of iron–porphyrins in organic solvents are discussed in the following text.

We propose that the occurrence of redox equilibria such as that described by Equation (5) may, under specific conditions, determine the nature of the iron–porphyrin observed as the final product of [Fe^{III}(P)] oxidation. With regard to the water-soluble complex **1**, we further suggest that the final product derived from reaction with ROOH at a given pH may differ from that initially formed by O–O bond cleavage in [Fe^{III}(P)(OOR)]. If, for example, $\mathbf{1}^{++}$ is formed by the reaction of **1** with a strong oxidant at pH > 7, it will tend to decay to $\mathbf{1}^{+}$ (the thermodynamically favored redox form at this pH). Because at pH > 7 $E^{\circ\prime}_{Fe^{IV}/Fe^{III}} < E^{\circ\prime}_{P^{\bullet+}/P}$ and $K_{disp} \ll 1$, this may occur through comproportionation [Eq. (5)]. Alternatively, $\mathbf{1}^{++}$ may decay to $\mathbf{1}^{+}$ through other redox reactions involving **1** [Eq. (6a)] or other components of the system [Eq. (6b)].

$$2\,[Fe^{IV}(P^{\bullet+})(O)] \rightarrow [Fe^{IV}(P)(O)] + \text{oxidatively decomposed } \mathbf{1} \quad (6a)$$

$$[Fe^{IV}(P^{\bullet+})(O)] + D \rightarrow [Fe^{IV}(P)(O)] + D^+ \qquad (D = \text{electron donor}) \quad (6b)$$

Particularly explicit examples of redox processes changing the nature of the oxidized iron–porphyrin formed by initial O–O bond cleavage, and their important influence on the subsequent catalytic activity, can be found in studies on the redox and catalytic properties of [Fe^{III}(P)] centers in heme oxygenases and in metmyoglobin.[21,25] As indicated by these studies, binding of ROOH to [Fe^{III}(P)] in peroxidases is followed by heterolytic O–O bond cleavage to form [Fe^{IV}-($P^{\bullet+}$)(O)]. This product is relatively stable in the absence of a reducing substrate, and was characterized by various spectroscopic techniques.[21,25b,c] In contrast, oxidation of the similar histidine-ligated [Fe^{III}(P)] center in metmyoglobin by various ROOH invariably led to [Fe^{IV}(P)(O)] being formed in a single kinetically observable step, initially suggesting that homolytic O–O bond cleavage occurs with this hemoprotein.[25d,h] However, subsequent studies revealed that the O–O bond in the [Fe(P)(OOR)] intermediate formed by metmyoglobin in reactions with *m*CPBA, H_2O_2, or organic peroxides undergoes heterolytic cleavage to give [Fe^{IV}-($P^{\bullet+}$)(O)]. The latter is then rapidly reduced to [Fe^{IV}(P)(O)]

by an imidazole residue of histidine (His64) present in the proximity of the heme.[25d,h,i] A similar instability of [Fe^{IV}-($P^{\bullet+}$)(O)] formed by initial heterolytic O–O bond cleavage in the presence of easily oxidizable amino acid residues in the surrounding heme has been demonstrated for a number of other hemoproteins.[25d–f] The rate of such subsequent redox steps (which determines the lifetime of the initially formed [Fe^{IV}($P^{\bullet+}$)(O)]) is greatly influenced by the type and location of amino acids that may act as reductants toward the oxidized heme.[25d–h]

For model [Fe^{III}(P)] complexes that lack the protein envelope, conversion of an initially formed oxidation product to other species may [in addition to reactions with external reductants, Eq. (6b)] easily involve the interaction of two [Fe(P)] molecules [Eqs. (5) and (6a)], if these processes are favored by the redox thermodynamics. For the reactions of **1** with *m*CPBA, H_2O_2, and PhIO in aqueous methanol reported here, a comproportionation reaction following the initial formation of $\mathbf{1}^{++}$ may indeed be expected at pH > 7.5. In the coordinating solvent used, the *K* value for the binding of the oxidant to **1** will be small,[26] with the coordination pre-equilibrium shown in Equation (7) shifted strongly to the left.

$$\begin{array}{l}[Fe^{III}(P)(L)] + ROOH \underset{H^+, L}{\overset{K}{\rightleftharpoons}} [Fe^{III}(P)(OOR)] \longrightarrow [Fe^{IV}(P^{\bullet+})(O)] \\ \qquad\qquad\qquad\qquad\qquad\qquad\qquad\qquad\qquad\qquad \Big\downarrow +[Fe^{III}(P)(L)] \\ L = RO^- \text{ or } 2ROH \qquad\qquad\qquad\qquad\qquad\qquad 2\,[Fe^{IV}(P)(O)]\end{array} \quad (7)$$

Because $E^{\circ\prime}_{Fe^{IV}/Fe^{III}} < E^{\circ\prime}_{P\cdot+/P}$ at pH > 7, [Fe^{III}(P)] (the predominant form in equilibrium *K*) will act as a reductant toward [Fe^{IV}($P^{\bullet+}$)(O)] if the latter is formed by heterolytic O–O bond cleavage at this pH, leading to the formation of [Fe^{IV}(P)(O)] as the final oxidation product.

In view of the above stated points, the observed reaction pattern for chemical oxidation of **1** in the pH range 4–10 can be interpreted as follows. Oxidation of **1** by *m*CPBA, PhIO, and H_2O_2 in the pH range 4–5.5 involves heterolysis of the O–O bond (or O–I bond in the case of PhIO) leading to the formation of $\mathbf{1}^{++}$. In the intermediate pH range, 5.5–7.5, the reaction may still involve O–O bond heterolysis.[27] However, irrespective of the actual bond cleavage mode, the final iron–porphyrin products formed in this pH range comprise a mixture of $\mathbf{1}^{++}$ and $\mathbf{1}^{+}$. Their relative concentrations at a given pH are determined by the pH-dependent equilibrium [Eq. (5)]. At pH > 7.5, $\mathbf{1}^{+}$ is the sole final product. This product may be formed by direct O–O bond homolysis in [Fe^{III}(P)(OOR)] (a reaction mode favored by a low $E^{\circ\prime}_{Fe^{IV}/Fe^{III}}$ value), or (in the case of initial $2e^-$ oxidation of **1**) through a subsequent comproportionation step, which is thermodynamically favored at this pH. Our experimental results obtained under catalytic conditions (oxidation of *cis*-stilbene by *m*CPBA in the presence of **1**) are consistent with these conclusions, because a change in the nature of the oxidized iron–porphyrin from $\mathbf{1}^{++}$ at pH 5 to $\mathbf{1}^{+}$ at pH 8 would be expected to drastically lower the catalytic activity of the system, as is indeed observed experimentally.[28] We furthermore propose that pH-dependent equilibria analogous to those discussed here for **1** may also be responsible for reported changes in the catalytic activities of other water-soluble iron(III)–porphyrins.[5m,n]

Factors influencing the redox properties of [Fe^{III}(P)] in nonaqueous solvents. Significance for mechanistic studies on O–O bond activation: The $E^{\circ\prime}$ versus pH profile in Figure 4 nicely visualizes the changes in the relative positions of $E^{\circ\prime}_{Fe^{IV}/Fe^{III}}$ and $E^{\circ\prime}_{P\cdot+/P}$ as a function of [H^+] for complex **1**. Electrochemical studies on water-insoluble [Fe^{III}(P)] in organic solvents cannot provide analogous data because 1) a convenient pH scale cannot be applied and 2) the oxo ligand is not available in electrochemical oxidations in dry organic solvents.[29] Nevertheless, careful consideration of literature data reported for such systems reveals a number of analogies with the diagram in Figure 4. Firstly, proton sensitivity of $E^{\circ\prime}_{Fe^{IV}/Fe^{III}}$ in nonaqueous media analogous to that observed for **1** can be inferred from the reported studies (see below). This is not surprising in view of the different abilities of O^{2-} and its protonated forms OH^- and H_2O to stabilize the Fe^{IV} center. Because this ability decreases in the order $O^{2-} \gg HO^- \gg H_2O$,[30–41] H^+-dependent stabilization of the oxo ligand in [Fe^{IV}(P)(O)] or [Fe^{IV}($P^{\bullet+}$)(O)] (which may be converted to OH^- or H_2O at high [H^+]) is expected to affect the relative positions of $E^{\circ\prime}_{Fe^{IV}/Fe^{III}}$ and $E^{\circ\prime}_{P\cdot+/P}$ in organic solvents in an analogous manner to that depicted for **1** in Figure 4.

We have shown for complex **1** that pH-induced changes in $E^{\circ\prime}_{Fe^{IV}/Fe^{III}}$ and $E^{\circ\prime}_{P\cdot+/P}$ may result in pH-dependent redox interconversions of high-valent iron–porphyrins. A good illustration of similar H^+-dependent redox equilibria in organic solvents may be found in studies on the hydrated iron–porphyrin radical [Fe^{III}($tmp^{\bullet+}$)(H_2O)(X)] (X = ClO_4^- or H_2O) in CH_2Cl_2 at −70 °C reported by Latos-Grazynski et al.[14] In these studies, addition of the proton scavenger 2,4,6-collidine (equivalent to an increase in pH in Figure 4) induced disproportionation of [Fe^{III}($tmp^{\bullet+}$)(H_2O)(X)] to [Fe^{IV}-($tmp^{\bullet+}$)(O)(X)] and [Fe^{III}(tmp)(OH)] (a shift from Section I to Section II in Figure 4).

$$\begin{array}{l}2\,[Fe^{III}(P^{\cdot+})(H_2O)(X)] + 3\,coll \rightarrow \\ \qquad [Fe^{IV}(P^{\cdot+})(O)(X)] + [Fe^{III}(P)(OH)] + 3\,collH^+ + X\end{array} \quad (8)$$

Sawyer et al.[42] reported redox interconversions corresponding to shifts between all three sections in Figure 4.

$$\begin{array}{ccc}[Fe^{IV}(P^{\bullet+})(O)] & \xrightarrow{OH^-} & [Fe^{IV}(P)(O)] \\ \text{Section II} & & \\ \Big\downarrow H^+ & & H^+\Big\uparrow \text{ Section III} \\ [Fe^{III}(P^{2+})(H_2O)] & & [Fe^{III}(P^{\bullet+})(H_2O)] \\ \text{Section I} & & \text{Section I}\end{array} \quad (9)$$

Goff et al.[40] observed disproportionation of $[Fe^{IV}(P)(F)_2]$ to $[Fe^{IV}(P^{\bullet+})(O)]$ in the presence of water, which served as a donor of O^{2-} and protons [Eq. (10)].

$$\underset{\text{Section III}}{2\,[Fe^{IV}(P)(F)_2]} \xrightarrow[2HF]{H_2O} \underset{\text{Section II}}{[Fe^{IV}(P^{\bullet+})(O)]} + [Fe^{III}(P)(F)_2] \qquad (10)$$

Other examples can be found in the literature for various $[Fe^{III}(P)]$ systems.[28b,35,43]

As mentioned above, the influence of pH on the relative positions of $E^{\circ\prime}_{Fe^{IV}/Fe^{III}}$ and $E^{\circ\prime}_{P^{\bullet+}/P}$ observed for **1** can be traced to different stabilization of Fe^{IV} by O^{2-}, HO^-, and H_2O. In this sense, it reflects a more general phenomenon observed for iron–porphyrin complexes: the strong influence of axial ligation on the stabilization of higher oxidation states of Fe (indicated experimentally by numerous electrochemical studies,[32,33,38,41,43–45] and further substantiated by theoretical calculations).[30,36,39,46–48] Electrochemical studies on [Fe(P)(X)] in organic solvents have clearly shown that X may influence the relative positions of $E^{\circ\prime}_{Fe^{IV}/Fe^{III}}$ and $E^{\circ\prime}_{P^{\bullet+}/P}$ by varying the degree of Fe^{IV} stabilization in the oxidized iron–porphyrin complex. When X is a weak ligand (e.g., ClO_4^- or $CF_3SO_3^-$), the relationship $E^{\circ\prime}_{Fe^{IV}/Fe^{III}} \gg E^{\circ\prime}_{P^{\bullet+}/P}$ was found experimentally.[32,33,49] The introduction of ligands offering moderate stabilization of Fe^{IV} (e.g., Cl^-, F^-, OH^-, imidazoles[36,37]) was found to lower the $E^{\circ\prime}_{Fe^{IV}/Fe^{III}}$ potential, such that $E^{\circ\prime}_{Fe^{IV}/Fe^{III}} \approx E^{\circ\prime}_{P^{\bullet+}/P}$.[38,43,44,50] Finally, when considerable stabilization of Fe^{IV} was offered by strong σ (or σ+π) donors (e.g., in the presence of an R^- group[41] or two axial CH_3O^- or F^- ligands), $E^{\circ\prime}_{Fe^{IV}/Fe^{III}} \ll E^{\circ\prime}_{P^{\bullet+}/P^{\bullet}}$.[32,40,41] We propose the schematic diagram shown in Figure 5 to visualize these general trends.[51] In analogy to the $E^{\circ\prime}$ versus pH profile in Figure 4, the diagram in Figure 5 can be divided into three sections, with the corresponding lowest-potential oxidations for each section being as indicated in Equations (11)–(13).[51]

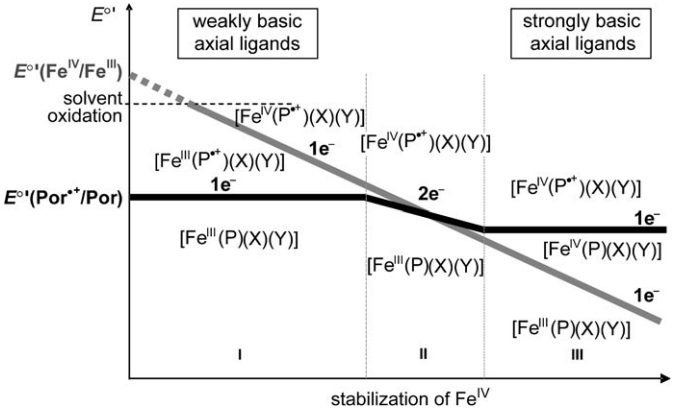

Figure 5. Schematic representation of the dependence of $E^{\circ\prime}_{Fe^{IV}/Fe^{III}}$ and $E^{\circ\prime}_{P^{\bullet+}/P}$ on the nature of the axial ligands in iron–porphyrin complexes.

$$\text{Section I } (E^{\circ\prime}_{Fe^{IV}/Fe^{III}} > E^{\circ\prime}_{P^{\bullet+}/P})$$
$$[Fe^{III}(P)(X)(Y)] \rightarrow [Fe^{III}(P^{\bullet+})(X)(Y)] + e^- \qquad (11)$$

$$\text{Section II } (E^{\circ\prime}_{Fe^{IV}/Fe^{III}} \approx E^{\circ\prime}_{P^{\bullet+}/P})$$
$$[Fe^{III}(P)(X)(Y)] \rightarrow [Fe^{IV}(P^{\bullet+})(X)(Y)] + 2\,e^- \qquad (12)$$

$$\text{Section III } (E^{\circ\prime}_{Fe^{IV}/Fe^{III}} < E^{\circ\prime}_{P^{\bullet+}/P})$$
$$[Fe^{III}(P)(X)(Y)] \rightarrow [Fe^{IV}(P)(X)(Y)] + e^- \qquad (13)$$

As previously discussed for **1**, the redox properties of [Fe(P)(X)] outlined in Figure 5 imply that the final products formed by chemical oxidation of [Fe(P)(X)] by ROOH in organic solvents do not necessarily reflect the actual mode of O–O bond cleavage, but their formation may involve subsequent redox processes [Eqs. (5)–(7)]. Thus, oxidation of [Fe(P)(X)] bearing a strongly basic ligand X that offers good stabilization of the Fe^{IV} center (i.e., a complex from Section III in Figure 5) by a strong oxidant with $E^{\circ\prime} > E^{\circ\prime}_{P^{\bullet+}/P} > E^{\circ\prime}_{Fe^{IV}/Fe^{III}}$ may initially give $[Fe^{IV}(P^{\bullet+})(O)(X)]$, which is then converted to $[Fe^{IV}(P)(O)(X)]$ through comproportionation [Eq. (7)]. The kinetics and thermodynamics of the latter process will be tuned by axial iron ligation, which determines the difference $E^{\circ\prime}_{Fe^{IV}/Fe^{III}} - E^{\circ\prime}_{P^{\bullet+}/P}$. To provide support for the assumption that the nature of X may indeed tune such equilibria, we oxidized $[Fe^{III}(tmp)(CF_3SO_3)]$ (**2**) (Figure 1) with *m*CPBA in CH_2Cl_2 at −40 °C and observed the formation of $[Fe^{IV}(tmp^{\bullet+})(O)(CF_3SO_3)]$ (**2**$^{++}$, λ = 396 nm, 600–700 nm;[7a,52] see Figure S5a in the Supporting Information). Subsequent addition of excess F^- resulted in conversion of **2**$^{++}$ to $[Fe^{IV}(tmp)(O)(F)]$ (**2**$^{+}$) (assigned on the basis of its UV/Vis spectrum; λ = 416 nm (Soret) and 545 nm;[35] Figure S5b). This experiment can be visualized in the diagram of Figure 5 as a shift from Section II ($X = O^{2-}$, $Y = CF_3SO_3^-$, $E^{\circ\prime}_{Fe^{IV}/Fe^{III}} \geq E^{\circ\prime}_{P^{\bullet+}/P}$) to Section III ($X = O^{2-}$, $Y = F^-$, $E^{\circ\prime}_{Fe^{IV}/Fe^{III}} < E^{\circ\prime}_{P^{\bullet+}/P}$) due to a change in the axial ligation of iron(IV). Further examples corresponding to analogous shifts between Sections I, II, and III upon changing the axial ligands can be widely found in the relevant literature. For example, Groves et al.[53] reported disproportionation of $[Fe^{III}(tmp^{\bullet+})(ClO_4)_2]$ to a mixture of $[Fe^{IV}(tmp^{\bullet+})(O)]$ and $[Fe^{III}(tmp)(L)]$ upon addition of 1 equiv of CH_3O^- (shift I→II in Figure 5; L denotes anionic ligands available in the system), while addition of excess CH_3O^-, OH^-, or CN^- resulted in conversion of $[Fe^{III}(tmp^{\bullet+})(ClO_4)_2]$ to $[Fe^{IV}(tmp)(L)_2]$ (shift I→III in Figure 5). In another study,[28b] conversion of $[Fe^{III}(tmp^{\bullet+})(ClO_4)_2]$ to $[Fe^{IV}(tmp)(O)(L)]$ (shift I→III in Figure 5) by ligand metathesis in the presence of wet basic alumina was reported.

We believe that the schematic diagram shown in Figure 5 could provide an explanation for the reported significant influence of the axial ligand X on the chemical oxidations of $[Fe^{III}(P)(X)]$ by *m*CPBA, PhIO, or H_2O_2 in nonaqueous solvents. As recently reported,[5j,k] such oxidations performed on selected $[Fe^{III}(P)(X)]$ in toluene, CH_2Cl_2, or CH_3CN/CH_2Cl_2 mixtures gave $[Fe^{IV}(P^{\bullet+})(O)(X)]$ when $X = ClO_4^-$, $CF_3SO_3^-$ or CH_3CN,[54] whereas with $X = Cl^-$, F^-, OH^- or

AcO^-, the $1e^-$-oxidized $[Fe^{IV}(P)(O)(X)]$ was formed. A change in the mode of O–O (or O–I) bond cleavage in the $[Fe^{III}(P)]$-bound oxidant, from heterolysis with $X = ClO_4^-$ or $CF_3SO_3^-$ to homolysis with $X = Cl^-$, F^-, OH^- or AcO^-,[5j,k] was suggested to explain this observation. It may be proposed on the basis of the diagram in Figure 5 that the iron–porphyrin product formed in the reaction with an oxidant does not necessarily reflect the mode of the initial O–O bond cleavage, but may represent the thermodynamically most stable redox form of the oxidized porphyrin (determined by the relative positions of $E^{\circ\prime}_{P^{\bullet+}/P}$ and $E^{\circ\prime}_{Fe^{IV}/Fe^{III}}$) under the given experimental conditions. In this context, the studied systems can be related to the schematic diagram in Figure 5 by considering the stabilization of the Fe^{IV} center in $[Fe^{IV}(P^{\bullet+})(O)(X)]$ by O^{2-} and X. An O^{2-} ligand is known to offer efficient stabilization of Fe^{IV},[30,31] and this can be further modified by X. When X is a weak ligand (such as ClO_4^-, $CF_3SO_3^-$, or CH_3CN), axial ligation by O^{2-} and X is likely to result in a moderate stabilization of Fe^{IV}, such that $E^{\circ\prime}_{Fe^{IV}/Fe^{III}} \geq E^{\circ\prime}_{P^{\bullet+}/P}$. Under such conditions, $[Fe^{IV}(P^{\bullet+})(O)(X)]$ is stabilized by the redox thermodynamics [Eqs. (5) and (5c)]. When, however, X provides somewhat better stabilization of Fe^{IV} (as expected for Cl^-, F^-, OH^-, and AcO^-),[31] $E^{\circ\prime}_{Fe^{IV}/Fe^{III}}$ will be lowered, and axial coordination by O^{2-} and X^- is likely to induce the condition $E^{\circ\prime}_{Fe^{IV}/Fe^{III}} \ll E^{\circ\prime}_{P^{\bullet+}/P}$. In this case, even if there is initial $2e^-$ oxidation of [Fe(P)(X)] to $[Fe^{IV}(P^{\bullet+})(O)(X)]$ in the reaction with ROOH, the latter will tend to decay to $[Fe^{IV}(P)(O)(X)]$ through comproportionation [Eq. (7)].

We further suggest that consideration of redox equilibria involving interconversions of high-valent iron–porphyrins may, in certain cases, be important for proper interpretation of experimental data obtained in mechanistic studies on [Fe(P)(X)]-catalyzed oxygenations (particularly when such studies are performed under catalytic conditions and the actual catalytically active iron–porphyrin form is not amenable to direct observation but must be inferred from indirect experimental evidence). Two general cases shown in Scheme 2 can be considered as possible complications in the interpretation of mechanistic studies performed under catalytic conditions when redox equilibria are operative.

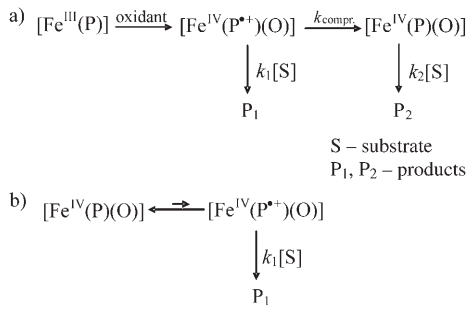

Scheme 2. Possible reaction pathways involving redox interconversions of high-valent oxo–iron–porphyrins under catalytic conditions ($[Fe^{III}(P)]$ + ROOH + substrate).

Scheme 2a refers to conditions under which a redox equilibrium following initial O–O bond cleavage strongly favors one of the high-valent iron–porphyrin forms (a condition that may be encountered when $E^{\circ}_{Fe^{IV}/Fe^{III}}$ and $E^{\circ}_{P/P^{\bullet+}}$ differ markedly, such that equilibrium according to Equation (5) is shifted toward one of the products). Because the reactivities of the immediate and final catalyst forms ($[Fe^{IV}(P^{\bullet+})(O)]$ and $[Fe^{IV}(P)(O)]$ in Scheme 2a) toward an organic substrate are usually very different,[28] the scheme implies that the nature and distribution of oxidized products formed from a substrate will be determined by the ratio $k_1[S]/k_{compr.}$ (which may vary greatly, depending on S and the actual reaction conditions determining $k_{compr.}$). Scheme 2b refers to conditions under which the redox thermodynamics moderately favors one of the iron–porphyrin forms resulting from [Fe(P)(X)] oxidation by ROOH. In such cases, the concentration of species that are catalytically active toward S may be low (and may elude experimental observation when oxidation of $[Fe^{III}(P)(X)]$ by ROOH is studied in the absence of S). Ambiguities can then arise when the nature of the high-valent iron–porphyrin catalytically active toward S is assessed by combination of the results obtained in the presence and absence of S. Notably, an example of a catalytic system involving a "discrete" catalytic activity of $[Fe^{IV}(tmp^{\bullet+})(O)]$ formed in small amounts by partial disproportionation of $[Fe^{IV}(tmp)(O)]$ has been reported previously.[28b]

Conclusion

Studies on model $[Fe^{III}(P)]$ complexes in solution have shown that the mechanism of O–O bond activation can be influenced by many factors. Principally, these include solvent polarity,[6a,b] the type of porphyrin ligand,[5,6a,b,7a] side reactions (e.g., with the solvent or excess oxidant),[3,5p,9,55] the reaction temperature,[5o] and the type of oxidant used.[3,6] The important influences of the acidity of the medium and the nature of the axial ligand in [Fe(P)(X)] on the rate and mechanism of O–O bond cleavage in [Fe(P){(H)OOR}] intermediates have also been recognized. The pH-dependence has usually been interpreted in terms of general acid/general base catalysis of ROOH coordination and heterolytic O–O bond cleavage, while the influence of X has often been ascribed to a "push effect".[6a,b]

Interpretation of the reactivity patterns reported in the present work has been focused on consideration of [Fe(P)(X)] and an oxidant (ROOH) as redox partners, which (after initial formation of the [Fe(P){(H)OOR}] intermediate) undergo an inner-sphere redox step involving $1e^-$ (O–O bond homolysis) or $2e^-$ (O–O bond heterolysis) iron–porphyrin oxidation. In this context, the redox characteristics of [Fe(P)(X)] with regard to oxidation to high-valent iron–porphyrin forms, and its sensitivity to $[H^+]$ and axial iron ligation, have been considered. Analysis of our own and other reported data with reference to the schematic diagrams shown in Figures 4 and 5 leads us to suggest that the acidity of the medium and axial iron ligation may influ-

ence the rate and mode of O–O bond cleavage, as well as the nature of the final products of [Fe(P)(X)] oxidation observed under given experimental conditions, by tuning the relative positions of $E^{\circ\prime}_{Fe^{IV}/Fe^{III}}$ and $E^{\circ\prime}_{P^{\bullet+}/P}$.

With regard to the catalytic efficiency of model $[Fe^{III}(P)(X)]$/ROOH systems in the hydroxylation and epoxidation of organic substrates, the presented results suggest that stereospecific, two-electron (enzyme-mimetic) oxygenations by $[Fe^{IV}(P^{\bullet+})(O)(X)]$ may be favored by judicious choice of reaction conditions (with regard to $[H^+]$ and/or the nature of X) under which $E^{\circ\prime}_{Fe^{IV}/Fe^{III}}$ is close to (or moderately higher than) $E^{\circ\prime}_{P^{\bullet+}/P}$ for a given catalytic system. Under such conditions, heterolytic O–O bond cleavage in the [Fe(P)]-bound peroxide may be favored by the porphyrin catalyst, and $[Fe^{IV}(P^{\bullet+})(O)(X)]$ is the thermodynamically stabilized oxidized form of [Fe(P)(X)]. In contrast, under experimental conditions favoring a large difference between $E^{\circ\prime}_{Fe^{IV}/Fe^{III}}$ and $E^{\circ\prime}_{P^{\bullet+}/P}$ (e.g., $E^{\circ\prime}_{Fe^{IV}/Fe^{III}} \ll E^{\circ\prime}_{P^{\bullet+}/P}$ for complex **1** at high pH), $1e^-$-oxidized iron–porphyrin forms are likely to be formed as final products of [Fe(P)(X)] oxidation. The latter, however, are not efficient in enzyme-mimetic catalytic oxygenations involving oxygen-transfer reactions.[59]

Experimental Section

Materials: The iron–porphyrins [*meso*-tetrakis(2,4,6-trimethyl-3-sulfonatophenyl)porphyrinato] (TMPS), iron(III) hydrate (sodium salt), and [*meso*-tetrakis(2,4,6-trimethylphenyl)porphyrinato] (TMP) iron(III) hydroxide were purchased from Frontier Scientific Ltd. Fine Chemicals, Utah (USA), and were used as received. *m*CPBA (75%, Acros Organics) was purified by sequential washing with phosphate buffer (pH 7.4) and water, followed by recrystallization from *n*-heptane. PhIO was synthesized from iodobenzene diacetate according to a literature method.[56] H_2O_2 (35% aqueous solution) was purchased from Fluka. Methanol (99.9%, Merck) and dichloromethane (99.99%, Fisher Chemicals) were used as received. MES, EPPS, and CAPS buffers were purchased from Sigma-Aldrich. *tert*-Butylammonium hydroxide (TBAOH, 30-hydrate, 98%) and *tert*-butylammonium fluoride (TBAF, 3-hydrate, 97%) were purchased from Fluka. Deionized water was used for the preparation of aqueous solutions. All other chemicals used in this study were of analytical reagent grade.

Measurements: pH measurements were performed with a Metrohm 623 pH meter that had been calibrated with standard aqueous buffer solutions. ^{1}H NMR spectra were measured on a Bruker Avance DPX-300 NM spectrometer. UV/Vis spectra were recorded on a Shimadzu UV-2100 spectrophotometer. Low-temperature time-resolved UV/Vis spectra were recorded with a Hi-Tech SF-3 L low-temperature stopped-flow unit (Hi-Tech Scientific, Salisbury, U.K.) equipped with a J&M TIDAS 16/300–1100 diode-array spectrophotometer (J&M, Aalen, Germany).

Spectroscopic measurements: Spectrophotometric titration of **1** in MeOH/H_2O (4:1, v/v) was performed at room temperature. HNO_3 and NaOH were used for pH adjustments. Time-resolved UV/Vis spectra were recorded by mixing an iron–porphyrin solution buffered to the desired pH ([buffer] = 0.02 M) with a freshly prepared oxidant solution at −35 °C in the low-temperature stopped-flow unit and following the absorbance changes. In order to minimize hydrolysis of *m*CPBA at pH > 6 and decomposition of PhIO, unbuffered solutions of these oxidants were freshly prepared before each measurement and adjusted to pH 5. Blank experiments performed at room temperature at each studied pH value indicated that the originally adjusted pH in the buffered iron–porphyrin solution did not change upon mixing with a solution of *m*CPBA or PhIO in a 1:1 ratio. In experiments involving H_2O_2, buffered solutions of iron–porphyrin and oxidant adjusted to the same pH value were used.

Measurement of the catalytic activity of $[Fe^{III}(tmps)]$ in the epoxidation of *cis*-stilbene: *m*CPBA (30 μL, dissolved in acetone) was slowly added in 3 μL aliquots to a solution of **1** (5×10^{-4} M) and *cis*-stilbene (5×10^{-2} M) in 1:1 MeOH/H_2O (0.47 mL) buffered at pH 5 (0.1 M acetate buffer) to give a final concentration of 1×10^{-2} M. A transient color change (from orange-brown to bright-green) following each addition of *m*CPBA indicated the formation of $[Fe^{IV}(tmps^{\bullet+})(O)]$ as the catalytically active species at this pH. The reaction mixture was vigorously stirred during addition of the oxidant, and for a further 10 min thereafter. The organic content of the sample was then extracted with chloroform (7 mL). The solvent was evaporated from the extract and the residue was redissolved in $CDCl_3$ (0.7 mL) containing $Si(Me)_4$ as an NMR reference. Subsequent NMR measurements indicated the presence of *cis*-stilbene oxide (δ = 4.37 ppm, s, 2H). The absence of a signal at δ = 3.86 ppm (s, 2H) indicated that no *trans*-stilbene oxide had been formed in the reaction. The yield of *cis*-stilbene oxide (60% with respect to the amount of *m*CPBA used) was calculated from the relative integrals of the ^{1}H NMR signals of *cis*-stilbene oxide at δ = 4.37 ppm and unreacted *cis*-stilbene (δ = 6.6 ppm, s, 2H). The aforementioned experimental procedure was then followed at pH 8.2 (EPPS buffer, 0.1 M[57]). In this case, no significant change in the greenish-yellow color of the solution of $[Fe^{III}(tmps)(OR)]$ (R = H, CH_3) was observed upon addition of *m*CPBA, indicating that $[Fe^{IV}(tmps^{\bullet+})(O)]$ was not formed in substantial amounts at this pH.[58] Experiments at both pH values were performed in duplicate to assure reproducibility of the results.

Acknowledgements

The authors gratefully acknowledge financial support from the Deutsche Forschungsgemeinschaft as part of SPP 1181.

[1] a) P. R. Ortiz de Montellano (Ed.), *Cytochrome P450: Structure, Mechanism and Biochemistry*, Plenum, New York, **1995**; b) M. Sono, M. P. Roach, E. D. Coulter, J. H. Dawson, *Chem. Rev.* **1996**, *96*, 2841.

[2] K. M. Kadish, K. M. Smith, R. Guilard (Eds.), *The Porphyrin Handbook, Vol. 4*, Academic Press, San Diego, **2000**.

[3] B. Meunier, *Chem. Rev.* **1992**, *92*, 1411.

[4] a) K. U. Ingold, P. A. MacFaul, in *Biomimetic Oxidations Catalyzed by Transition Metal Complexes* (Ed.: B. Meunier), Imperial College Press, London, **2000,** pp. 45–89; b) J. McLain, J. Lee, J. T. Groves, in *Biomimetic Oxidations Catalyzed by Transition Metal Complexes* (Ed.: B. Meunier), Imperial College Press, London, **2000**, pp. 91–169.

[5] a) W. J. Song, Y.-J. Sun, S. K. Choi, W. Nam, *Chem. Eur. J.* **2006**, *12*, 130; b) W. J. Song, Y. O. Ryu, R. Song, W. Nam, *J. Biol. Inorg. Chem.* **2005**, *10*, 294; c) W. Nam, Y. O. Ryu, W. J. Song, *J. Biol. Inorg. Chem.* **2004**, *9*, 654; d) W. Nam, S.-E. Park, I. K. Lim, M. H. Lim, J. Hong, J. Kim, *J. Am. Chem. Soc.* **2003**, *125*, 14674; e) W. Nam, S.-Y. Oh, Y. J. Sun, J. Kim, W.-K. Kim, S. K. Woo, W. Shin, *J. Org. Chem.* **2003**, *68*, 7903; f) W. Nam, S. W. Jin, M. H. Lim, J. Y. Ryu, Ch. Kim, *Inorg. Chem.* **2002**, *41*, 3647; g) W. Nam, M. H. Lim, S. K. Moon, Ch. Kim, *J. Am. Chem. Soc.* **2000**, *122*, 10805; h) W. Nam, M. H. Lim, H. J. Lee, Ch. Kim, *J. Am. Chem. Soc.* **2000**, *122*, 6641; i) W. Nam, H. J. Lee, S.-Y. Oh, Ch. Kim, H. G. Jang, *J. Inorg. Biochem.* **2000**, *80*, 219; j) W. Nam, M. H. Lim, S.-Y. Oh, *Inorg. Chem.* **2000**, *39*, 5572; k) W. Nam, M. H. Lim, S.-Y. Oh, J. H. Lee, H. J. Lee, S. K. Woo, Ch. Kim, W. Shin, *Angew. Chem.* **2000**, *112*, 3792; *Angew. Chem. Int. Ed.* **2000**, *39*, 3646; l) Y. M. Goh, W. Nam, *J. Am. Chem. Soc.* **1999**, *121*, 914; m) W. Nam, H. J. Choi, H. J. Han, S. H. Cho, H. J. Lee, S.-Y. Han, *Chem. Commun.* **1999**, 387; n) S. J. Yang, W. Nam, *Inorg. Chem.* **1998**, *37*, 606; o) K. A. Lee, W. Nam, *J. Am. Chem. Soc.* **1997**, *119*, 1916; p) W. Nam, H. J. Han, S.-Y. Oh, Y. J. Lee, M. H. Choi, S.-Y. Han, Ch. Kim, S. K. Woo, W. Shin, *J. Am. Chem. Soc.* **2000**, *122*, 8677.

[6] a) K. Machii, Y. Watanabe, I. Morishima, *J. Am. Chem. Soc.* **1995**, *117*, 6691, and references therein; b) K. Yamaguchi, Y. Watanabe, I.

Morishima, *J. Am. Chem. Soc.* **1993**, *115*, 4058; c) Y. Watanabe, K. Yamaguchi, I. Morishima, K. Takehira, M. Shimizu, T. Hayakawa, H. Orita, *Inorg. Chem.* **1991**, *30*, 2582; d) J. T. Groves, Y. Watanabe, *J. Am. Chem. Soc.* **1988**, *110*, 8443; e) R. Labeque, L. J. Marnett, *J. Am. Chem. Soc.* **1989**, *111*, 6621.

[7] a) H. Fujii, *J. Am. Chem. Soc.* **1993**, *115*, 4641; b) F. Minisci, F. Fontana, S. Araneo, F. Recupero, S. Banfi, S. Quici, *J. Am. Chem. Soc.* **1995**, *117*, 226; c) Z. Gross, S. Nimri, *Inorg. Chem.* **1994**, *33*, 1731; d) N. Suzuki, T. Higuchi, T. Nagano, *J. Am. Chem. Soc.* **2002**, *124*, 9622; e) T. Ohno, N. Suzuki, T. Dokoh, Y. Urano, K. Kikuchi, M. Hirobe, T. Higuchi, T. Nagano, *J. Inorg. Biochem.* **2000**, *82*, 123; f) D. Meyer, T. Leifels, L. Sbaragli, W. D. Woggon, *Biochem. Biophys. Res. Commun.* **2005**, *338*, 372; g) W. D. Woggon, H. A. Wagenknecht, C. Claude, *J. Inorg. Biochem.* **2001**, 83, 289.

[8] a) T. G. Traylor, Ch. Kim, W.-P. Fann, Ch. L. Perrin, *Tetrahedron*, **1998**, *54*, 7977; b) T. G. Traylor, Ch. Kim, J. L. Richards, F. Xu, C. L. Perrin, *J. Am. Chem. Soc.* **1995**, *117*, 3468; c) T. G. Traylor, S. Tsuchiya, Y.-S. Byun, Ch. Kim, *J. Am. Chem. Soc.* **1993**, *115*, 2775; d) T. G. Traylor, F. Xu, *J. Am. Chem. Soc.* **1990**, *112*, 178; e) T. G. Traylor, W.-P. Fann, D. Bandyopadhyay, *J. Am. Chem. Soc.* **1989**, *111*, 8009; f) T. G. Traylor, J. P. Ciccone, *J. Am. Chem. Soc.* **1989**, *111*, 8413; g) T. G. Traylor, F. Xu, *J. Am. Chem. Soc.* **1987**, *109*, 6201.

[9] a) Ö. Almarsson, T. C. Bruice, *J. Am. Chem. Soc.* **1995**, *117*, 4533; b) T. C. Bruice, *Acc. Chem. Res.* **1991**, *24*, 243, and references therein; c) G.-X. He, T. C. Bruice, *J. Am. Chem. Soc.* **1991**, *113*, 2747; d) M. F. Zipplies, W. A. Lee, T. C. Bruice, *J. Am. Chem. Soc.* **1986**, *108*, 4433.

[10] a) S. Jin, T. A. Bryson, J. H. Dawson, *J. Biol. Inorg. Chem.* **2004**, *9*, 644; b) S. Shaik, S. P. de Visser, D. Kumar, *J. Biol. Inorg. Chem.* **2004**, *9*, 661.

[11] a) M. Wolak, R. van Eldik, *J. Am. Chem. Soc.* **2005**, *127*, 13312; b) J.-E. Jee, M. Wolak, D. Balbinot, N. Jux, A. Zahl, R. van Eldik, *Inorg. Chem.* **2006**, *45*, 1326, and references therein.

[12] M. Liu, Y. O. Su, *J. Electroanal. Chem.* **1998**, *452*, 113.

[13] a) M. Liu, Ch. Yeh, Y. O. Su, *Chem. Commun.* **1996**, 1437; b) F.-Ch. Chen, J.-H. Ho, Ch.-Y. Chen, Y. O. Su, T.-I. Ho, *J. Electroanal. Chem.* **2001**, *499*, 17.

[14] K. Rachlewicz, L. Latos-Grazynski, *Inorg. Chem.* **1996**, *35*, 1136.

[15] A standard glass electrode was used to determine the apparent pH in the aqueous methanol solvent mixture.

[16] In the mixed solvent used, water and methanol, and their deprotonated forms OH^- and CH_3O^-, compete for coordination to the metal center in the "acidic" and "basic" porphyrin forms, respectively. However, only the overall pH-dependent equilibrium [Eq. (1b)] is important with regard to the aspects discussed in this report. The actual identity of the axial ligands in $[Fe^{III}(P)(HOR)_2]$ and $[Fe^{III}(P)(OR)]$ (water or methanol, HO^- or CH_3O^-) is of minor importance for the interpretation of the experimental results, and is therefore not addressed in any further detail.

[17] The UV/Vis spectral features of the product are very characteristic of $[Fe^{IV}(P^{+\bullet})(O)]$ species with an a_{2u} radical character.[7a] The spectrum of the product closely resembles that observed for the well-characterized $[Fe^{IV}(tmp^{+\bullet})(O)]$ complex.[7a] Its assignment as $[Fe^{IV}(tmps^{+\bullet})(O)]$ is consistent with that concluded by Su et al. on the basis of spectroelectrochemical studies on **1**.[12,13]

[18] J. F. Goodman, P. Robson, E. R. Wilson, *Trans. Faraday Soc.* **1962**, *58*, 1846.

[19] Slow kinetics of the reaction of **1** with $[H_2O_2]$ at $-35\,^\circ C$ necessitated the use of relatively concentrated solutions of this oxidant ($[H_2O_2] > 5\times10^{-2}$ M, ≈1000-fold excess over [**1**]). At such high H_2O_2 concentrations, interference of decomposition processes with spectral changes attributable to the initial reaction steps could not be avoided at pH < 6.

[20] Interestingly, a pH-dependent change in the nature of the high-valent iron–porphyrin similar to that reported here for the model complex **1** has also been observed in the reaction of *m*CPBA with His64 mutants of metmyoglobin.[25h] Further experimental data evidencing pH-induced differences in the stabilities of $[Fe^{IV}(P^{+\bullet})(O)]$ and $[Fe^{IV}(P)(O)]$ formed in the reactions of ROOH with metmyoglobin and peroxidases (pointing to increased stability of $[Fe^{IV}(P^{+\bullet})(O)]$ at low pH and of $[Fe^{IV}(P)(O)]$ at high pH) can be found in refs. [20a–c] and ref. [25b]; a) J.-S. Wang, H. K. Baek, H. E. Van Wart, *Biochem. Biophys. Res. Commun.* **1991**, *179*, 1320; b) Z. S. Farhangrazi, B. R. Copeland, T. Nakayama, T. Amachi, I. Yamazaki, L. S. Powers, *Biochemistry* **1994**, *33*, 5647; c) T. Egawa, S. Yoshioka, S. Takahashi, H. Hori, S. Nagano, H. Shimada, K. Ishimori, I. Morishima, M. Suematsu, *J. Biol. Chem.* **2003**, *278*, 41597.

[21] P. Jones, H. B. Dunford, *J. Inorg. Biochem.* **2005**, *99*, 2292.

[22] Five-coordinate $[Fe^{III}(P)(OOR)]$ complexes have been observed in a number of studies; see, for example: a) ref. [6b]; b) J. T. Groves, Y. Watanabe, *Inorg. Chem.* **1987**, *26*, 785; c) R. D. Arasasingham, Ch. R. Cornman, A. L. Balch, *J. Am. Chem. Soc.* **1989**, *111*, 7800; d) R. D. Arasasingham, A. L. Balch, L. Latos-Grazynski, *J. Am. Chem. Soc.* **1987**, *109*, 5846.

[23] a) The schematic diagram in Figure 4 refers to aqueous solution and was constructed on the basis of experimental data obtained from the detailed electrochemical studies on **1** reported in ref. [12]. The original $E^{\circ\prime}$ versus pH diagram is reproduced from ref. [12] as Figure S3 in the Supporting Information. Ref. [12] (provided as a pdf file as Supporting Information) also includes a detailed description of the redox properties of **1** based on cyclic voltammetric and spectroelectrochemical measurements; b) Potentials characterizing metal- and porphyrin-centered reductions, as well as $2e^-$ oxidation of the porphyrin ligand to the porphyrin dication, P^{2+}, have not been included in the diagram in Figure 4 as these processes are not relevant to the topics discussed in this report.

[24] The different values of $E^{\circ\prime}_{P^{+\bullet}/P}$ at pH < 3.5 (+0.930 V vs. Ag/AgCl)[12] and pH > 6.5 (+0.83 V)[12] are not the result of a direct pH-dependence, but rather reflect the influence of the Fe center (its axial ligation, oxidation state, and spin state) on the porphyrin-centered oxidation. In this context, it should be noted that oxidation of the porphyrin ligand at pH < 3.5 involves a $[Fe^{III}(P)(H_2O)_2]$ complex with an (almost purely high-spin)[11] Fe^{III} center coordinated by two axial H_2O ligands. In contrast, porphyrin-centered oxidation at pH > 6.5 involves a $[Fe^{IV}(P)(O)(H_2O)]$ complex, with an Fe^{IV} center ($S = 1$) coordinated by O^{2-} and H_2O. As the metal ion "communicates" electronically with the porphyrin ligand in most [Fe(P)(X)] complexes, small (usually < 200 mV) variations in $E^{\circ\prime}_{P^{+\bullet}/P}$ are often encountered upon a change in the axial ligation/spin state/oxidation state of Fe in [Fe(P)(X)] systems; see, for example, ref. [41a] (Table 1), refs. [41b,c]. The slope of a plot of $E^{\circ\prime}$ vs. pH observed for **1** at pH 4–7 ($-60\,mV\,pH^{-1}$) indicates a $2e^-$, $2H^+$ process. This pH dependence results from oxidation of Fe^{III} to Fe^{IV} being accompanied by conversion of the H_2O ligand to O^{2-}, that is, it is associated with a metal-centered redox transition (which cannot be separated from the ligand-centered redox wave due to the small difference between $E^{\circ\prime}_{P^{+\bullet}/P}$ and $E^{\circ\prime}_{Fe^{IV}/Fe^{III}}$ in this pH range; cf. ref. [12]). In this context, description of the porphyrin-centered oxidation of **1** as "relatively pH-insensitive" seems fully justified.

[25] a) Interestingly, $E^{\circ\prime}$ vs. pH profiles reported for the imidazole-ligated high-spin heme of peroxidases in the pH range 5–11[25b] closely resemble that presented in Figure 4 for complex **1** in this pH range, indicating similar general trends in the pH-dependent redox properties of $[Fe^{III}(P)]$ in both peroxidases and model complex **1**. A pH-dependence of $E^{\circ\prime}_{Fe^{IV}/Fe^{III}}$ similar to that observed for **1** has also been reported for the [Fe(P)] center of metmyoglobin;[25j] b) Y. Hayashi, I. Yamazaki, *J. Biol. Chem.* **1979**, *254*, 9101; c) A. N. P. Hiner, E. L. Raven, R. N. F. Thorneley, F. Garcia-Canovas, J. N. Rodriguez-Lopez, *J. Inorg. Biochem.* **2002**, *91*, 27; d) S.-I. Ozaki, M. P. Roach, T. Matsui, Y. Watanabe, *Acc. Chem. Res.* **2001**, *34*, 818; e) A. Ivancich, Ch. Jakopitsch, M. Auer, S. Un, Ch. Obinger, *J. Am. Chem. Soc.* **2003**, *125*, 14093; f) G. M. Jensen, S. W. Bunte, A. Warshel, D. B. Goodin, *J. Phys. Chem. B* **1998**, *102*, 8221; g) A. Morimoto, M. Tanaka, S. Takahashi, K. Ishimori, H. Hori, I. Morishima, *J. Biol. Chem.* **1998**, *273*, 14753; h) T. Matsui, S.-I. Ozaki, Y. Watanabe, *J. Biol. Chem.* **1997**, *272*, 32735; i) T. Matsui, S.-I. Ozaki, Y. Watanabe, *J. Am. Chem. Soc.* **1999**, *121*, 9952; j) P. George, D. H. Irvine, *Biochem. J.* **1955**, *60*, 596.

[26] MeOH and H_2O are relatively weak ligands for the Fe^{III} centers of $[Fe^{III}(P)]$.[26a,b] As the binding strengths of the O-donor ligands *m*CPBA, PhIO, and H_2O_2 are expected to be similar or lower compared to those of MeOH and H_2O, and the latter are present in large excess, very small K values are indeed expected for initial ROOH (or PhIO) coordination to **1** when water or aqueous methanol is used as solvent. a) A. Hoshino, Y. Ohgo, M. Nakamura, *Inorg. Chem.* **2005**, *44*, 7333; b) D. R. Evans, Ch. A. Reed, *J. Am. Chem. Soc.* **2000**, *122*, 4660.

[27] $E^{\circ\prime} \approx +1.15$ V (vs. $Ag/AgCl_{sat}$) can be calculated for H_2O_2 (the weakest oxidant used in this study) at pH 7. This value is higher than $E^{\circ\prime}_{Fe^{IV}/Fe^{III}}$ and $E^{\circ\prime}_{P^{\bullet+}/P}$ determined for **1** at this pH (see Figure 4 and ref. [12]). Thus, $2e^-$ oxidation is very likely to occur at pH 5.5–7.5 with H_2O_2 and other (stronger) oxidants used in this study.

[28] a) Low catalytic activity and mechanistically distinct characteristics of epoxidations catalyzed by $1e^-$-oxidized $[Fe^{IV}(P)(O)]$ forms of synthetic iron–porphyrins as compared to $2e^-$-oxidized $[Fe^{IV}(P^{\bullet+})(O)]$ are well documented.[28b–e] Conversion of $[Fe^{IV}(P^{\bullet+})(O)]$ centers to $[Fe^{IV}(P)(O)]$/protein radical pairs in redox reactions with easily oxidizable amino acid residues in the proximity of heme has also been observed to influence the catalytic activity of heme oxygenases.[25d–h] b) J. T. Groves, Z. Gross, M. K. Stern, *Inorg. Chem.* **1994**, *33*, 5065; c) J. T. Groves, R. C. Haushalter, M. Nakamura, T. E. Nemo, B. J. Evans, *J. Am. Chem. Soc.* **1981**, *103*, 2884; d) R. Labeque, L. J. Marnett, *J. Am. Chem. Soc.* **1989**, *111*, 6621; e) G.-X. He, T. C. Bruice, *J. Am. Chem. Soc.* **1991**, *113*, 2747.

[29] Unless the $[Fe^{III}(P)(X)]$ porphyrin is introduced as a hydroxo complex or residual water is present in the system.

[30] J. Conradie, J. C. Swarts, A. Ghosh, *J. Phys. Chem. B* **2004**, *108*, 452.

[31] On the basis of various spectroscopic, electrochemical, and theoretical studies, the order of the degree of Fe^{IV} stabilization by X is roughly as follows: ClO_4^-, $CF_2SO_3^-$, NO_3^-[32,33] < MeOH, H_2O,[12,14,34,35] imidazoles[36,37] < Cl^-, F^-,[38,39] HO^-,[30,38] CH_3O^-[32,35] < $2F^-$,[39,40] $2CH_3O^-$,[30,32,35] R^-[41] < O^{2-}.[30]

[32] K. M. Kadish, E. van Caemelbecke, G. Royal, in *The Porphyrin Handbook, Vol. 8* (Eds.: K. M. Kadish, K. M. Smith, R. Guilard), Academic Press, San Diego, **2000**, Chapter 55, and references therein.

[33] A. D. Boersma, H. M. Goff, *Inorg. Chem.* **1984**, *23*, 1671.

[34] J. T. Groves, J. A. Gilbert, *Inorg. Chem.* **1986**, *25*, 125.

[35] J. T. Groves, R. Quinn, T. J. McMurry, G. Lang, B. Boso, *J. Chem. Soc. Chem. Commun.* **1984**, 1455.

[36] J. Conradie, A. Ghosh, *J. Phys. Chem. B* **2003**, *107*, 6486.

[37] a) T. Ikeue, Y. Ohgo, M. Nakamura, *Chem. Commun.* **2003**, 220; b) M. Nakamura, Y. Kawasaki, *Chem. Lett.* **1996**, 805.

[38] A. Nanthakumar, H. M. Goff, *Inorg. Chem.* **1991**, *30*, 4460.

[39] D. H. Jones, A. S. Hinman, T. Ziegler, *Inorg. Chem.* **1993**, *32*, 2092.

[40] D. L. Hickman, A. Nanthakumar, H. M. Goff, *J. Am. Chem. Soc.* **1988**, *110*, 6384.

[41] a) K. M. Kadish, E. Van Caemelbecke, F. D'Souza, C. J. Medforth, K. M. Smith, A. Tabard, R. Guilard, *Inorg. Chem.* **1995**, *34*, 2984; b) K. M. Kadish, E. Van Caemelbecke, E. Gueletti, S. Fukuzumi, K. Miyamoto, T. Suenobu, A. Tabard, R. Guilard, *Inorg. Chem.* **1998**, *37*, 1759; c) S. Fukuzumi, I. Nakanishi, K. Tanaka, T. Suenobu, A. Tabard, R. Guilard, E. Van Caemelbecke, K. M. Kadish, *J. Am. Chem. Soc.* **1999**, *121*, 785.

[42] H. Sugimoto, H.-Ch. Tung, D. T. Sawyer, *J. Am. Chem. Soc.* **1988**, *110*, 2465.

[43] W. A. Lee, T. S. Calderwood, T. C. Bruice, *Proc. Natl. Acad. Sci. USA* **1985**, *82*, 4301.

[44] a) T. S. Calderwood, W. A. Lee, T. C. Bruice, *J. Am. Chem. Soc.* **1985**, *107*, 8272; b) T. S. Calderwood, T. C. Bruice, *Inorg. Chem.* **1986**, *25*, 3722.

[45] L. A. Bottomley, K. M. Kadish, *Inorg. Chem.* **1981**, *20*, 1348.

[46] A. Ghosh, T. Vangberg, E. Gonzales, P. Taylor, *J. Porphyrins Phthalocyanines* **2001**, *5*, 345.

[47] D. L. Harris, *Curr. Opin. Chem. Biol.* **2001**, *5*, 724.

[48] M. T. Green, *J. Am. Chem. Soc.* **2000**, *122*, 9495.

[49] For $[Fe(P)(X)]$ complexes with very weakly binding X, the $E^{\circ}_{Fe^{IV}/Fe^{III}}$ potentials are high, and often lie above the upper electrochemical window of the solvent. As a result, only the redox waves associated with porphyrin-centered oxidations ($P \rightarrow P^{\bullet+}$ and $P^{\bullet+} \rightarrow P^{2+}$) can be measured experimentally.[32,33]

[50] For such complexes, redox waves for the $Fe^{III} \rightarrow Fe^{IV}$ and $P \rightarrow P^{\bullet+}$ transitions observed in cyclic voltammetric studies lie close together or merge into a single wave corresponding to a $2e^-$ oxidation of $[Fe^{III}(P)(X)]$ to $[Fe^{IV}(P^{\bullet+})(X)]$.[38,43,44]

[51] $[Fe^{III}(P)(X)(Y)]$ may be a five-coordinate (e.g., for $X = Cl^-$, CH_3O^-) or six-coordinate (e.g., $X = Y = CH_3OH$) complex; $[Fe^{III}(P^{\bullet+})(X)(Y)]$ and $[Fe^{IV}(P)(X)(Y)]$ are six-coordinate in the presence of ligands and/or in coordinating solvents.

[52] a) E. Bill, X.-Q. Ding, E. L. Bominaar, A. X. Trautwein, H. Winkler, D. Mandon, R. Weiss, A. Gold, K. Jayaraj, W. E. Hatfield, M. L. Kirk, *Eur. J. Biochem.* **1990**, *188*, 665; b) D. Mandon, R. Weiss, K. Jayaraj, A. Gold, J. Terner, E. Bill, A. X. Trautwein, *Inorg. Chem.* **1992**, *31*, 4404.

[53] J. T. Groves, R. Quinn, T. J. McMurry, M. Nakamura, G. Lang, B. Boso, *J. Am. Chem. Soc.* **1985**, *107*, 354.

[54] As pointed out in footnote [11] of ref. [5f], weakly coordinating counter ions such as $X = ClO_4^-$ or $CF_3SO_3^-$ in $[Fe(P)(X)]$ are substituted by acetonitrile when the latter is present as solvent. As $2e^-$ oxidation has been observed for $[Fe(P)(X)]$ with weakly binding counter ions X in CH_3CN/CH_2Cl_2 mixtures, acetonitrile is included in the set of ligands that promote $2e^-$ porphyrin oxidation.

[55] A. Gold, K. Jayaraj, P. Doppelt, R. Weiss, G. Chottard, E. Bill, X. Ding, A. X. Trautwein, *J. Am. Chem. Soc.* **1988**, *110*, 5756.

[56] H. Saltzman, J. G. Sharefkin, *Org. Synth., Collect. Vol. V*, Wiley, New York, **1973**, p. 658.

[57] In more dilute buffer solutions, gradual addition of *m*CPBA changed the sample color to orange-brown (identical to that observed for **1** at pH 5) and subsequently to bright-green. This resulted from a drop in pH upon introduction of higher concentrations of *m*CPBA ($>$ ca. 5×10^{-3} M) to the reaction mixture. In order to avoid ambiguities caused by instability of the solution pH, buffer concentrations of 0.1 M (at which no changes in pH upon addition of *m*CPBA were observed) were used at both of the pH values studied.

[58] Oxidation of *cis*-stilbene to *cis*-stilbene oxide was also observed in the absence of the [Fe(tmps)] catalyst at pH 5. The yield of the epoxide product was, however, significantly lower compared to that from the iron–porphyrin-catalyzed reaction under identical reaction conditions (18%, as compared to 60% in the presence of [Fe(tmps)]). Transient changes in the sample color upon each incremental addition of *m*CPBA in the case of the [Fe(tmps)]-catalyzed reaction indicate unequivocally that the oxo–iron–porphyrin radical is formed as the catalytically active species at lower pH. When PhIO was used as the oxidant under similar reaction conditions ([**1**] = 0.005 M, [PhIO] = 0.03 M, [*cis*-stilbene] = 0.05 M, [buffer] = 0.1 M, pH 5 ($AcOH/AcO^-$ buffer) or pH 8 (EPPS buffer)), a reactivity pattern fully analogous to that described for *m*CPBA was observed. At pH 5, $[Fe^{IV}(tmps^{\bullet+})(O)]$ was transiently formed as the catalytically active species, and *cis*-stilbene oxide was the sole oxidation product. Neither $[Fe^{IV}(tmps^{\bullet+})(O)]$ nor *cis*-stilbene oxide were observed in the catalytic reaction with PhIO at pH 8. The yields of *cis*-stilbene oxide formed at pH 5 were, however, significantly lower (ca. 8%) as compared to those obtained with *m*CPBA as the oxidant (60%).

[59] **Note added in proof** (05. 03. 07): Since the submission of this work we have found evidence that a gradual change of the oxidized iron–porphyrin product from $\mathbf{1}^{++}$ to $\mathbf{1}^{+}$ on increasing pH may be due to the reduction of $\mathbf{1}^{++}$ by OH^- at high pH. Further studies to evaluate this possibility are new in progress.

Received: August 9, 2006
Revised: November 24, 2006
Published online: March 16, 2007

